Pergamon

Int. J. Solids Structures Vol. 32, No. 3/4, pp. 515–523, 1995

0020–7683/95 $9.50 + .00

0020–7683(94)00128–6

DECAY OF STRESSES INDUCED BY SELF-EQUILIBRATED END LOADS IN A MULTILAYERED COMPOSITE

A. C. WIJEYEWICKREMA
Department of Civil Engineering, Northwestern University, Evanston, IL 60208, U.S.A.

(*Received* 23 *June* 1994)

Abstract—The axial decay of stresses induced by self-equilibrated end loads in a multilayered composite is investigated in the context of the plane problem. Here the multilayered composite is composed of alternating layers of two dissimilar isotropic materials. By adopting appropriate boundary conditions it is sufficient to consider a cell which consists of three layers. An Airy stress function approach is utilized to obtain the characteristic equation where the non-zero roots correspond to the decay rates. The dominant exponential decay rate, which corresponds to the smallest positive real part of the roots is presented in the Dundurs α, β parallelogram.

1. INTRODUCTION

Saint-Venant's principle, which is often used to simplify complications in the vicinity of applied loads, can be expressed as follows: "the difference between stress fields due to two statically equivalent applied loads is negligible at distances which are greater than the largest dimension of the area over which the loads are acting". This principle can also be stated as, "the effect of the stress field due to a self-equilibrated load is insignificant at distances away from the load". While this principle is in general valid for homogeneous isotropic elastic material, it has been shown that the characteristic decay length for composite structures could be quite different. Excellent reviews of the Saint-Venant effect in composite structures can be found in Horgan and Knowles (1983) and Horgan (1989). While much work has been reported for the problem of sandwich strips, very few studies have been carried out for multilayered composite structures.

The exact decay rates for plane problems of a sandwich strip composed of two dissimilar isotropic materials with perfect interfacial bonding was investigated by Choi and Horgan (1978). The exponential decay of end effects away from the loaded ends was characterized in terms of complex eigenvalues, analogous to the well-known Fadle–Papkovich eigenvalues for the homogeneous isotropic strip. Finite element methods have been applied to problems of sandwich strips by Rao and Valsarajan (1980), Okumura *et al.* (1985) and Goetschel and Hu (1985). A recent investigation by Wijeyewickrema *et al.* (1994) has exploited the results of Dundurs (1969) on the reduced dependence on elastic constants for plane deformation of two phase composites. They give comprehensive results for the symmetric and anti-symmetric cases, for various ratios of volume fractions in the α, β plane, where α, β are the Dundurs constants. The effect of slipping interfaces on the exponential decay of end effects in a sandwich strip was studied by Wijeyewickrema (1994). The characteristic equations obtained for the symmetric and anti-symmetric cases were shown to depend only on the single composite parameter α, which agrees with the general properties of frictionless contact along a straight interface (Dundurs, 1975). In the present analysis the axial diffusion of self-equilibrated end loads in a multilayered composite is investigated.

To the author's knowledge analytical studies of Saint-Venant end effects in multilayered composites have not been carried out previously. The only attempt at studying

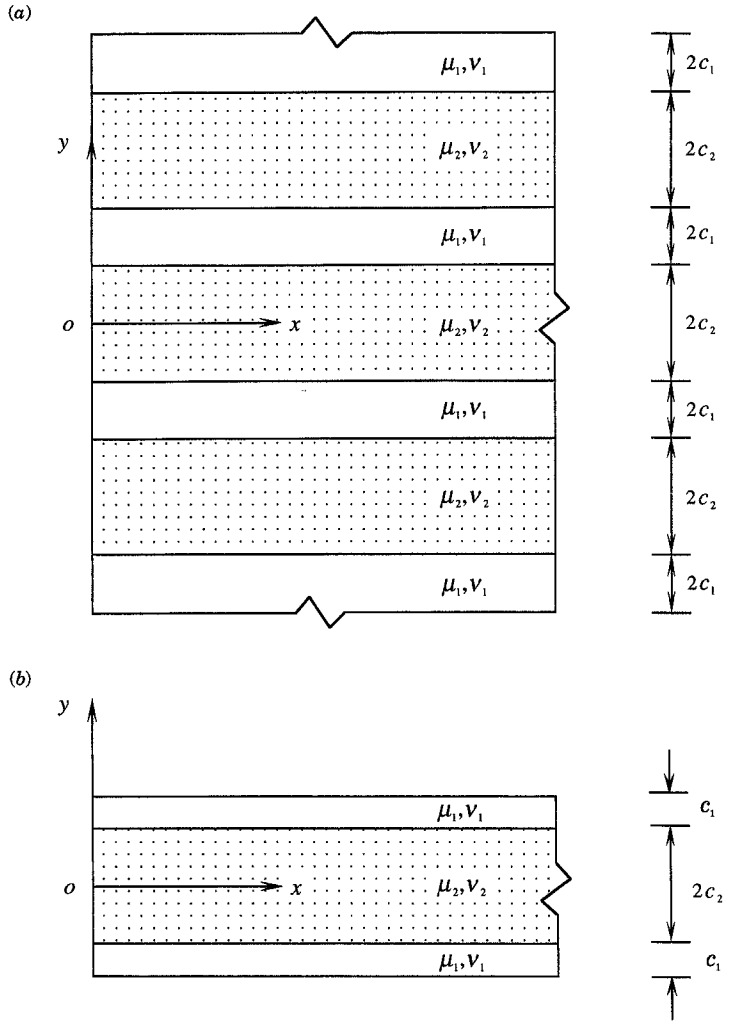

Fig. 1. (a) Multi-layered composite composed of alternating layers of dissimilar material. (b) Representative cell used in analysis.

this problem was the work reported by Dong and Goetschel (1982), who investigated the end effects on laminated composite plates by means of the finite element method. Laminated plates composed of an arbitrary number of bonded anisotropic elastic layers were studied using this numerical approach.

In the next section the problem is formulated and the characteristic equation which yields the decay rates is obtained in terms of the Dundurs constants. The dominant exponential decay rate for the stresses is given by the real part of the eigenvalue with the smallest, positive real part. The results are discussed in detail in section 3, where decay rates of self-equilibrating end loads are plotted in the α, β plane.

2. FORMULATION OF THE PROBLEM

The semi-infinite multilayered composite shown schematically in Fig. 1(a) consists of two dissimilar alternating layers of homogeneous isotropic material with elastic constants μ_i, ν_i $(i = 1, 2)$ and thickness $2c_i$ $(i = 1, 2)$. Here μ_i, ν_i are the shear modulus and Poisson's ratio, respectively. The layers are perfectly bonded at the interfaces. The volume fraction f of material '1', is defined as the ratio of the thickness of the layer '1' to the thickness of the unit cell,

$$f = \frac{2c_1}{2c_1 + 2c_2}. \tag{1}$$

In the present analysis only symmetric deformations of the multilayered composite are considered, i.e. each layer is assumed to be loaded by self-equilibrated loads which are symmetric about its own mid-plane. Hence, due to considerations of symmetry, it is sufficient to consider a representative cell which consists of three layers, as shown in Fig. 1(b). Since $y = 0$ is a plane of symmetry, in what follows only the upper half of the representative cell $y \geqslant 0$ is considered. The displacements and stresses in each layer can be obtained by means of the Fadle–Papkovich functions (Timoshenko and Goodier, 1970, p. 62), which exhibit exponential decay in the axial direction, and are given in the Appendix.

The stresses in the two dissimilar layers are of the form

$$\sigma_{ij}^1(x, y) = \mathrm{e}^{-x_1} f_{ij}^1(y), \quad x_1 = \gamma_1 x / c_1 \tag{2}$$

and

$$\sigma_{ij}^2(x, y) = \mathrm{e}^{-x_2} f_{ij}^2(y), \quad x_2 = \gamma_2 x / c_2, \tag{3}$$

where the superscripts and subscripts 1, 2 refer to material 1 and material 2, respectively. The objective of this analysis is to investigate the effect of different material combinations on the decay rates γ_1/c_1 and γ_2/c_2.

The perfect bonding assumed at the interface results in the continuity conditions

$$\begin{aligned} &\sigma_{yy}^1(x, c_2) = \sigma_{yy}^2(x, c_2), \quad \sigma_{xy}^1(x, c_2) = \sigma_{xy}^2(x, c_2), \quad 0 \leqslant x < \infty \\ &u_x^1(x, c_2) = u_x^2(x, c_2), \quad u_y^1(x, c_2) = u_y^2(x, c_2), \quad 0 \leqslant x < \infty \end{aligned} \tag{4}$$

and the boundary conditions on the external surface of the representative cell are taken as

$$\sigma_{xy}^1(x, c_1 + c_2) = 0, \quad u_y^1(x, c_1 + c_2) = 0, \quad 0 \leqslant x < \infty, \tag{5}$$

due to the symmetric deformation of the multi-layered composite.

The interfacial conditions (4) and the periodicity conditions on the external surface of the representative cell [eqn (5)], yield a system of six equations for the six unknown coefficients associated with the displacement and stress fields. The determinant of the coefficients, which characterizes the exponential decay rates in the multi-layered composite, is obtained as

$$\begin{aligned} \Delta_s(\gamma; \alpha, \beta, f) = {} & \alpha^2[a_1 + \gamma^2] + 2\alpha\{-\beta[f\gamma a_2 + (1-f)\gamma a_3] + [f\gamma a_2 - (1-f)\gamma a_3]\} \\ & + \{\beta^2 a_2 a_3 - 2\beta[f\gamma a_2 - (1-f)\gamma a_3] - a_4\}, \end{aligned} \tag{6}$$

where

$$\begin{aligned} a_1 &= \sin^2(1-2f)\gamma - (1-2f)^2\gamma^2, \quad a_2 = \sin 2(1-f)\gamma + 2(1-f)\gamma, \\ a_3 &= \sin 2f\gamma + 2f\gamma, \qquad\qquad a_4 = \sin^2\gamma. \end{aligned} \tag{7}$$

Here,

$$\alpha = \frac{\Gamma(\kappa_1 + 1) - (\kappa_2 + 1)}{\Gamma(\kappa_1 + 1) + (\kappa_2 + 1)}, \quad \beta = \frac{\Gamma(\kappa_1 - 1) - (\kappa_2 - 1)}{\Gamma(\kappa_1 + 1) + (\kappa_2 + 1)}, \tag{8}$$

are the constants introduced by Dundurs (1969), where $\Gamma = \mu_2/\mu_1$, $\kappa_i = 3 - 4\nu_i$, for plane

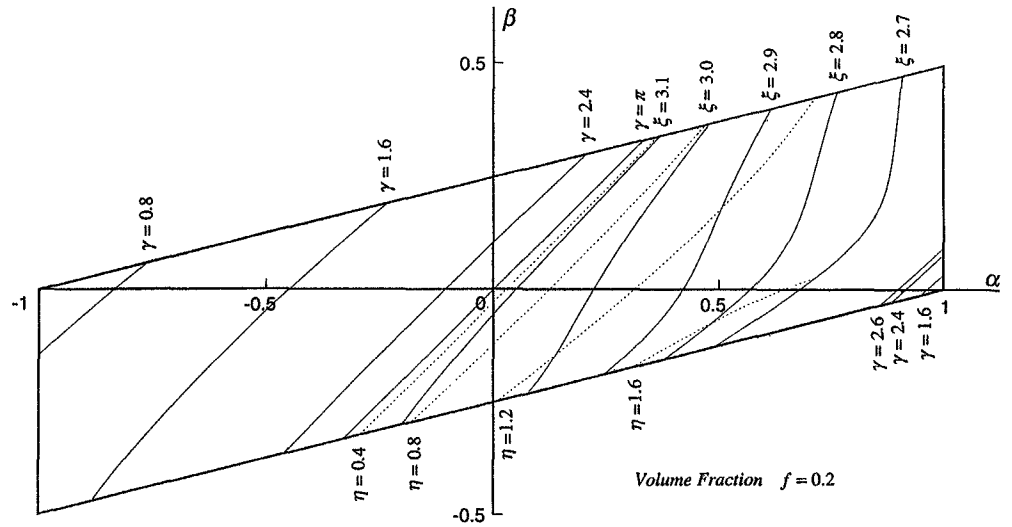

Fig. 2. Roots of $\Delta_s(\gamma;\alpha,\beta,f)=0$, which correspond to the smallest, positive real part of $\gamma=\xi+i\eta$, for $f=0.2$.

strain and $\kappa_i=(3-\nu_i)/(1+\nu_i)$, $(i=1,2)$ for generalized plane stress. Under the usual physical assumptions of $\mu_i>0$, and $0\leqslant\nu_i\leqslant 1/2$, the admissible values of α and β are restricted to a parallelogram in the α, β plane, with $-1\leqslant\alpha\leqslant 1$ and $-1/2\leqslant\beta\leqslant 1/2$.

The eigenvalue γ introduced in eqn (6) to compare the exponential decay rate γ_1/c_1 with that for a homogeneous unit cell of the same total thickness is defined by

$$\frac{\gamma}{c_1+c_2}=\frac{\gamma_1}{c_1}. \tag{9}$$

The application of interfacial conditions given by eqn (4) results in

$$\frac{\gamma_1}{c_1}=\frac{\gamma_2}{c_2}. \tag{10}$$

It is noted that Δ_S has a complicated structure in the variables f and γ, but is simply quadratic in the material constants α and β.

3. RESULTS AND DISCUSSION

The roots of the transcendental equation $\Delta_S(\gamma;\alpha,\beta,f)=0$ are analyzed here to obtain the exponential decay rate for the stresses. It is noted that the dominant decay rate for the stresses is the real part of the eigenvalue γ with the smallest, positive real part. The roots of $\Delta_S(\gamma;\alpha,\beta,f)=0$ are determined numerically and plotted in Figs 2–6, for $f=0.2$, 0.4, 0.5, 0.6 and 0.8 in the α,β parallelogram. For a given volume fraction f, when γ is real, a root is chosen and its locus is plotted in the α,β plane by solving the quadratic in α for each β in the range $-1/2\leqslant\beta\leqslant 1/2$. When γ is complex we express γ as $\gamma=\xi+i\eta$ and write

$$\Delta_S(\xi+i\eta;\alpha,\beta,f)=\Delta_S^R(\xi,\eta;\alpha,\beta,f)+i\Delta_S^I(\xi,\eta;\alpha,\beta,f) \tag{11}$$

and solve the two quadratics in α to obtain ξ,η curves.

In general these figures are obtained by combining plots of complex roots and real roots. This is illustrated for the volume fraction $f=0.6$ in Fig. 5(a–c). The complex roots $\gamma=\xi+i\eta$ are plotted as contours $\xi=$ constant, $\eta=$ constant in Fig. 5(a) and the real roots γ are plotted as contours $\gamma=$ constant in Fig. 5(b). In Fig. 5(a), the thick line corresponds to the curve $\eta=0$ and the lower end point of the curve $\xi=\pi$ has an imaginary part $\eta=0$.

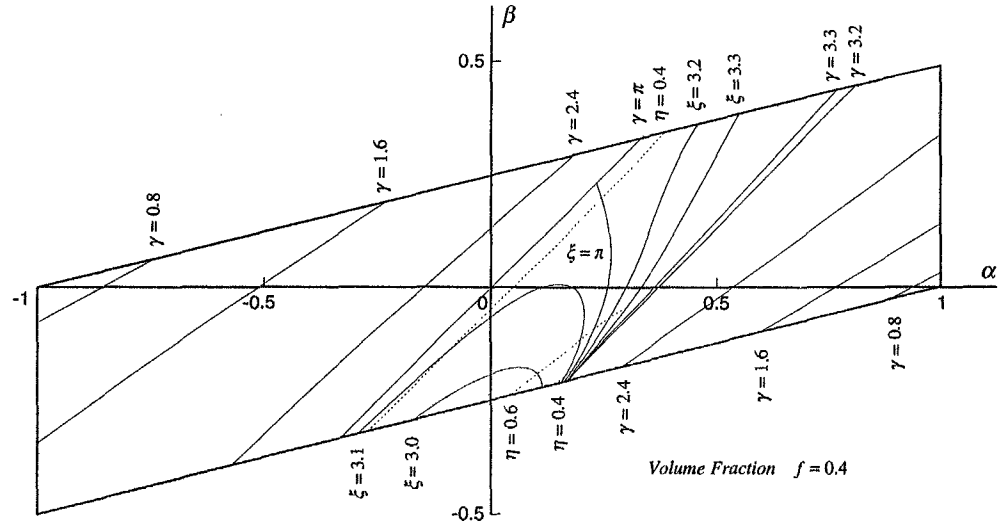

Fig. 3. Roots of $\Delta_s(\gamma\,;\alpha,\beta,f)=0$, which correspond to the smallest, positive real part of $\gamma=\xi+i\eta$, for $f=0.4$.

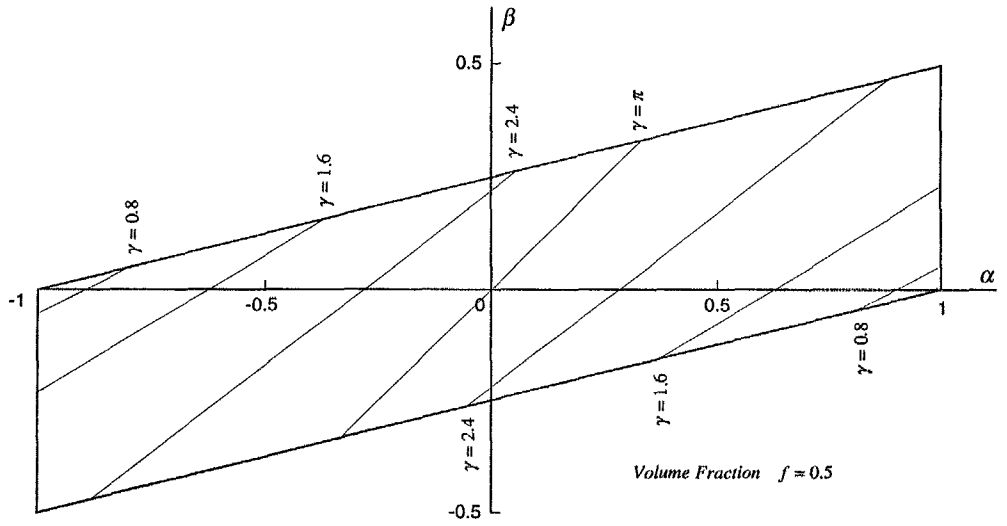

Fig. 4. Roots of $\Delta_s(\gamma\,;\alpha,\beta,f)=0$, which correspond to the smallest, positive real part of $\gamma=\xi+i\eta$, for $f=0.5$.

Figures 5(a), and 5(b) are combined to get Fig. 5(c) which represent the roots with the smallest, positive real part of γ. The set of complex roots belonging to the family with $\xi<4.0$ has a definite pattern which is easily observed from Fig. 5(a), while the sets of complex roots belonging to other families with $\xi>4.0$ do not show readily recognizable patterns. Thus note, that when $\xi>4.0$, the $\eta=$ constant curves may intersect each other and the $\xi=$ constant curves may intersect the $\eta=0$ curve.

From Figs 2 and 3 it is observed that, when $f<0.5$, the decay rates always correspond to real roots to the left of the line $\gamma=\pi$ and in the vicinity of $\alpha=1$. For the volume fraction $f=0.5$, no complex roots were found and the decay rates correspond to real roots in the entire α,β parallelogram (see Fig. 4). This is expected, since when $f=0.5$ eqn (6) yields

$$\Delta_S(\gamma\,;\alpha,\beta,0.5)=\alpha^2\gamma^2-2\alpha\beta\gamma(\sin\gamma+\gamma)+\{\beta^2(\sin\gamma+\gamma)^2-\sin^2\gamma\},\tag{12}$$

which defines real roots for constant γ along the straight lines

$$\alpha = [\beta(\sin\gamma + \gamma) \pm \sin\gamma]/\gamma. \tag{13}$$

When $f > 0.5$, Figs 5 and 6 indicate that the decay rates correspond always to real roots to the right of the line $\gamma = \pi$ and in the vicinity of $\alpha = -1$. When the alternating layers consist of identical material, i.e. when $\alpha = \beta = 0$, the characteristic equation is $\sin^2\gamma = 0$, and is independent of the volume fraction f. Thus in Figs 2–6 the curve $\gamma = \pi$ goes through the origin.

Due to the symmetric nature of the problem, the results for a particular volume fraction f can be obtained from the results for the volume fraction $(1-f)$ by reflection about the origin in the α, β plane. This is because the volume fraction f of material "1" corresponds to a volume fraction $(1-f)$ of material "2", and when the materials in the unit cell of Fig. 1(b) are interchanged, the constants α and β have to be replaced by $-\alpha$ and $-\beta$, respectively. This feature can be seen by comparing for instance, Fig. 2 with Fig. 6.

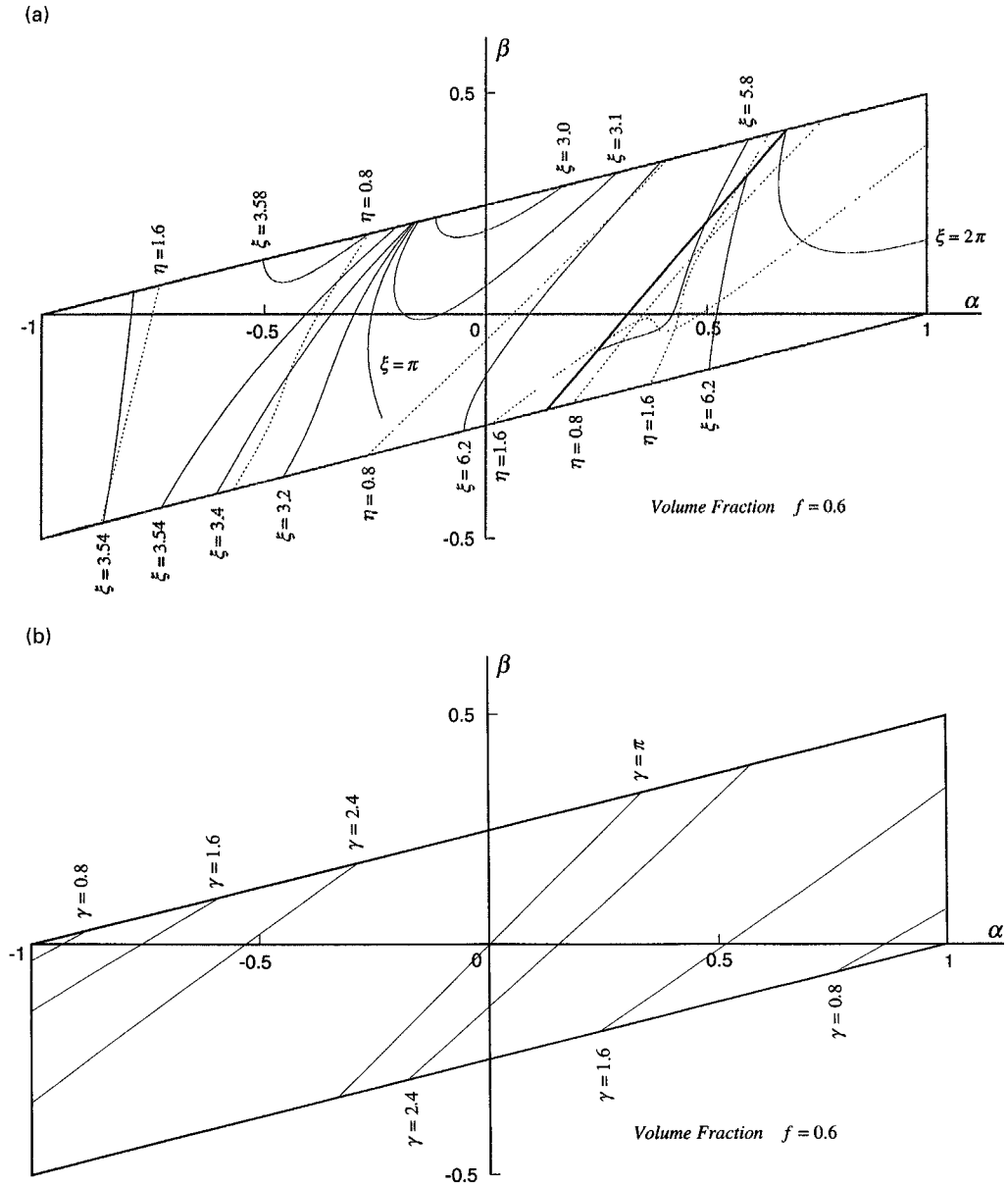

Fig. 5. Roots of $\Delta_s(\gamma; \alpha, \beta, f) = 0$, for $f = 0.6$. (a) Complex roots $\gamma = \xi + i\eta$, (b) real roots, and (c) roots which correspond to the smallest, positive real part of γ.

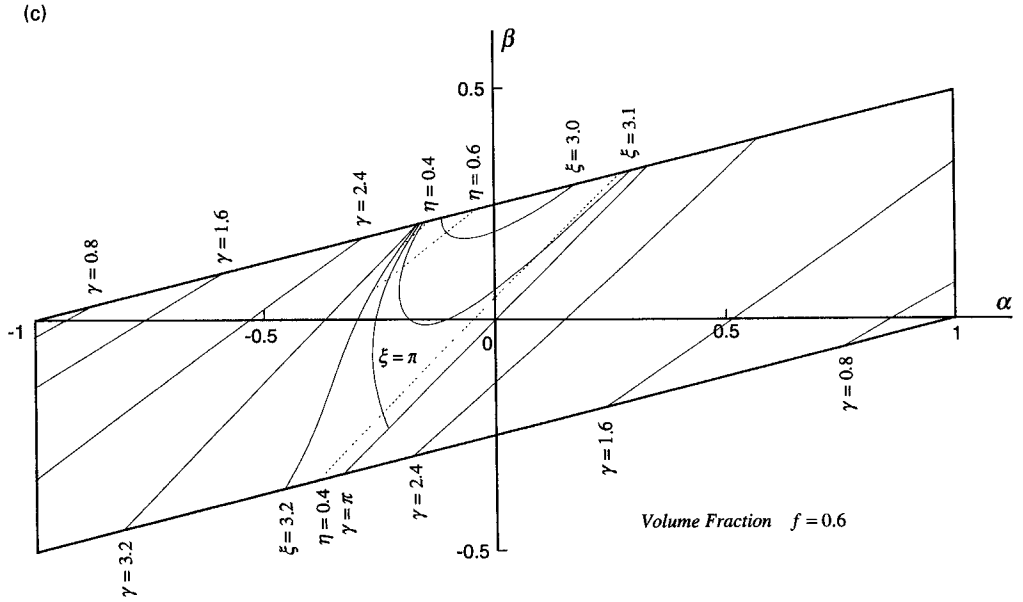

Fig. 5.—Continued.

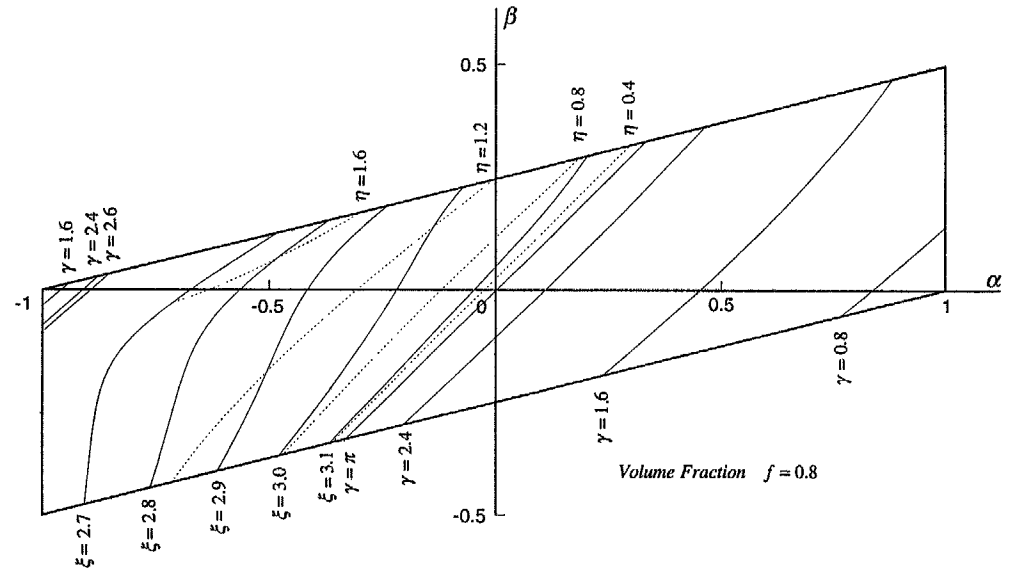

Fig. 6. Roots of $\Delta_s(\gamma; \alpha, \beta, f) = 0$, which correspond to the smallest, positive real part of $\gamma = \xi + i\eta$, for $f = 0.8$.

4. CONCLUDING REMARKS

The ideas of Dundurs regarding the reduced dependence on the elastic constants for two phase composites have been used to represent the decay of end effects in multilayered composites in an elegant manner. The results are presented in plots which are useful to designers. The analysis also serves as a benchmark for researchers using numerical methods.

Acknowledgments—The author's interest in Saint-Venant effects originated in conversations with Professor John Dundurs. Further discussions with Professors Dundurs and Cornelius O. Horgan resulted in a detailed analysis of the problem first considered by Choi and Horgan (1978). The author is pleased to acknowledge helpful discussions with Professors Dundurs and Leon Keer during the course of the work reported here.

REFERENCES

Choi, I. and Horgan, C. O. (1978). Saint-Venant end effects for plane deformation of sandwich strips. *Int. J. Solids Struct.* **14,** 187–195.

Dong, S. B. and Goetschel, D. B. (1982). Finite element analysis of edge effects in laminated composite plates. *ASME J. Appl. Mech.* **49,** 129–135.

Dundurs, J. (1969). Discussion. *ASME J. Appl. Mech.* **36,** 650–652.

Dundurs, J. (1975). Properties of elastic bodies in contact. *The Mechanics of the Contact Between Deformable Bodies* (Edited by A. D. de Pater and J. J. Kalker). Delft University Press, Delft.

Goetschel, D. B. and Hu, T. H. (1985). Quantification of Saint-Venant's principle for a general prismatic member. *Comput. Struct.* **21,** 869–874.

Horgan, C. O. (1989). Recent developments concerning Saint-Venant's principle: an update. *ASME Appl. Mech. Rev.* **42,** 295–303.

Horgan, C. O. and Knowles, J. K. (1983). Recent developments concerning Saint-Venant's principle. In *Advances in Applied Mechanics* Vol. 23 (Edited by J. W. Hutchinson), pp. 179–269. Academic Press, New York.

Okumura, H., Watanabe, K. and Yamada, J. (1985). Finite-element analyses of Saint-Venant end effects for composite materials. In *Recent Advances in Composites in the United States and Japan*, ASTM STP 864 (Edited by J. R. Vinson and M. Taya), pp. 225–235. ASTM, Philadelphia.

Rao, N. R. and Valsarajan, K. V. (1980). Saint-Venant's principle in sandwich strip. *Comput. Struct.* **12,** 185–188.

Timoshenko, S. P. and Goodier, J. N. (1970). *Theory of Elasticity*, 3rd edn. McGraw-Hill, New York.

Wijeyewickrema, A. C. (1994). Axial decay of stresses in a layered composite with slipping interfaces. In *Proc. First Int. Conf. Composites Engineering*, 28–31 August, 1994, New Orleans, LA.

Wijeyewickrema, A. C., Horgan, C. O. and Dundurs, J. (1994). Further analysis of the end effects in plane deformation of sandwich strips. Submitted to *ASME J. Appl. Mech.*

APPENDIX

The stresses and displacements in the outer layers are given by

$$\sigma_{xx}^1(x,y) = e^{[-(\gamma_1 x/c_1)]}\left(\frac{\gamma_1}{c_1}\right)\left\{-\cos\left(\frac{\gamma_1 y}{c_1}\right)A_1 - \left[\frac{\gamma_1 y}{c_1}\cos\left(\frac{\gamma_1 y}{c_1}\right)+2\sin\left(\frac{\gamma_1 y}{c_1}\right)\right]B_1 - \sin\left(\frac{\gamma_1 y}{c_1}\right)C_1 + \left[2\cos\left(\frac{\gamma_1 y}{c_1}\right) - \frac{\gamma_1 y}{c_1}\sin\left(\frac{\gamma_1 y}{c_1}\right)\right]D_1\right\}, \quad \text{(A1)}$$

$$\sigma_{yy}^1(x,y) = e^{[-(\gamma_1 x/c_1)]}\left(\frac{\gamma_1}{c_1}\right)\left\{\cos\left(\frac{\gamma_1 y}{c_1}\right)A_1 + \frac{\gamma_1 y}{c_1}\cos\left(\frac{\gamma_1 y}{c_1}\right)B_1 + \sin\left(\frac{\gamma_1 y}{c_1}\right)C_1 + \frac{\gamma_1 y}{c_1}\sin\left(\frac{\gamma_1 y}{c_1}\right)D_1\right\}, \quad \text{(A2)}$$

$$\sigma_{xy}^1(x,y) = e^{[-(\gamma_1 x/c_1)]}\left(\frac{\gamma_1}{c_1}\right)\left\{-\sin\left(\frac{\gamma_1 y}{c_1}\right)A_1 + \left[\cos\left(\frac{\gamma_1 y}{c_1}\right) - \frac{\gamma_1 y}{c_1}\sin\left(\frac{\gamma_1 y}{c_1}\right)\right]B_1 + \cos\left(\frac{\gamma_1 y}{c_1}\right)C_1 + \left[\frac{\gamma_1 y}{c_1}\cos\left(\frac{\gamma_1 y}{c_1}\right)+\sin\left(\frac{\gamma_1 y}{c_1}\right)\right]D_1\right\}, \quad \text{(A3)}$$

$$4\mu_1 u_x^1(x,y) = e^{[-(\gamma_1 x/c_1)]}\left\{2\cos\left(\frac{\gamma_1 y}{c_1}\right)A_1 + \left[2\frac{\gamma_1 y}{c_1}\cos\left(\frac{\gamma_1 y}{c_1}\right)+(1+\kappa_1)\sin\left(\frac{\gamma_1 y}{c_1}\right)\right]B_1 + 2\sin\left(\frac{\gamma_1 y}{c_1}\right)C_1 + \left[-(1+\kappa_1)\cos\left(\frac{\gamma_1 y}{c_1}\right)+2\frac{\gamma_1 y}{c_1}\sin\left(\frac{\gamma_1 y}{c_1}\right)\right]D_1\right\}, \quad \text{(A4)}$$

$$4\mu_1 u_y^1(x,y) = e^{[-(\gamma_1 x/c_1)]}\left\{2\sin\left(\frac{\gamma_1 y}{c_1}\right)A_1 + \left[(\kappa_1-1)\cos\left(\frac{\gamma_1 y}{c_1}\right)+2\frac{\gamma_1 y}{c_1}\sin\left(\frac{\gamma_1 y}{c_1}\right)\right]B_1 - 2\cos\left(\frac{\gamma_1 y}{c_1}\right)C_1 + \left[-2\frac{\gamma_1 y}{c_1}\cos\left(\frac{\gamma_1 y}{c_1}\right)+(\kappa_1-1)\sin\left(\frac{\gamma_1 y}{c_1}\right)\right]D_1\right\}, \quad \text{(A5)}$$

where A_1, B_1, C_1, D_1 are arbitrary constants.

The stresses and displacements in the inner layer for symmetric deformation of the inner layer can be expressed as

$$\sigma_{xx}^2(x,y) = e^{[-(\gamma_2 x/c_2)]}\left(\frac{\gamma_2}{c_2}\right)\left\{-\cos\left(\frac{\gamma_2 y}{c_2}\right)A_2 + \left[2\cos\left(\frac{\gamma_2 y}{c_2}\right) - \frac{\gamma_2 y}{c_2}\sin\left(\frac{\gamma_2 y}{c_2}\right)\right]D_2\right\}, \quad \text{(A6)}$$

$$\sigma_{yy}^2(x,y) = e^{[-(\gamma_2 x/c_2)]}\left(\frac{\gamma_2}{c_2}\right)\left\{\cos\left(\frac{\gamma_2 y}{c_2}\right)A_2 + \frac{\gamma_2 y}{c_2}\sin\left(\frac{\gamma_2 y}{c_2}\right)D_2\right\}, \quad \text{(A7)}$$

$$\sigma_{xy}^2(x,y) = e^{[-(\gamma_2 x/c_2)]}\left(\frac{\gamma_2}{c_2}\right)\left\{-\sin\left(\frac{\gamma_2 y}{c_2}\right)A_2+\left[\frac{\gamma_2 y}{c_2}\cos\left(\frac{\gamma_2 y}{c_2}\right)+\sin\left(\frac{\gamma_2 y}{c_2}\right)\right]D_2\right\}, \tag{A8}$$

$$4\mu_2 u_x^2(x,y) = e^{[-(\gamma_2 x/c_2)]}\left\{2\cos\left(\frac{\gamma_2 y}{c_2}\right)A_2+\left[-(1+\kappa_2)\cos\left(\frac{\gamma_2 y}{c_2}\right)+2\frac{\gamma_2 y}{c_2}\sin\left(\frac{\gamma_2 y}{c_2}\right)\right]D_2\right\}, \tag{A9}$$

$$4\mu_2 u_y^2(x,y) = e^{[-(\gamma_2 x/c_2)]}\left\{2\sin\left(\frac{\gamma_2 y}{c_2}\right)A_2+\left[-2\frac{\gamma_2 y}{c_2}\cos\left(\frac{\gamma_2 y}{c_2}\right)+(\kappa_2-1)\sin\left(\frac{\gamma_2 y}{c_2}\right)\right]D_2\right\}, \tag{A10}$$

where A_2, B_2, C_2, D_2 are arbitrary constants.